

Two-stage Robust Nash Bargaining-based Energy Trading between Hydrogen-enriched Gas and Active Distribution Networks

Wenwen Zhang, Gao Qiu, Hongjun Gao, *Member, IEEE*, Tingjian Liu, Junyong Liu, *Member, IEEE*, Yaping Li, Shengchun Yang, Jiahao Yan, Wenbo Mao

Abstract—Integration of emerging hydrogen-enriched compressed natural gas (HCNG) distribution network with active distribution network (ADN) provides huge latent flexibility on consuming renewable energies. However, paucity of energy trading mechanism risks the stable earnings of the flexibility for both entities, especially when rising highly-efficient solid oxide fuel cells (SOFCs) are pioneered to interface gas and electricity. To fill the gap, a two-stage robust Nash bargaining strategy is proposed. In the first stage, a privacy-preserved Nash Bargaining based on the ADMM is applied to clear energy trading between the two autonomous entities, i.e., ADN and gas distribution network (GDN). Via robust dispatch of configured energy storage in ADN, the next stage de-risks ADN's profit collapse from transaction biases, caused by forecasting errors of distributed energy resources. C&CG is finally utilized to loop the two stages. The convergence of the entire energy trading strategy is theoretically proved. As such, sustain-able returns from the integration of ADN and GDN bridged by SOFC and HCNG are facilitated. Numerical studies indicate that, the proposed cooperative strategy reaps a stable social welfare of nearly 1.6% to total cost, and benefit-steady situations for both ADN and GDN, even in the worst case.

Index Terms—Hydrogen enriched compressed natural gas, two-stage robust, Nash bargaining, solid oxide fuel cells, hybrid energy storage system, li-ion battery

NOMENCLATURE

A. Abbreviation

HCNG	Hydrogen-enriched compressed natural gas
IENGs	Integrated electricity and natural gas systems
ADN	Active distribution network
GDN	Gas distribution network
HGN	Higher-level gas network
P2G	Power to gas
G2P	Gas to power
DER	Distributed energy resource
ET	Electrolytic tank
HT	Hydrogen tank
SOFC	Solid oxide fuel cell
HESS	Hybrid energy storage system
C&CG	Column-and-constraint generation
ADMM	Alternating direction method of multipliers
BCD	Block coordinate descending

B. Sets/Indices

$\mathbb{J}_1/\mathbb{J}_2/\mathbb{J}_3/\mathbb{J}_4$	Set of P2Gs/ G2Ps/li-ion batteries/DERs
\mathbb{A}/\mathbb{B}	Set of nodes in GDN/ ADN
\mathbb{T}	Set of operation periods
$m/n/g$	Index of natural gas nodes
$i/j/h$	Index of power nodes

$j_1/j_2/j_3/j_4$
 t

Index of P2G/ G2P/ li-ion battery/ DER
Index of operation periods

C. Parameters

Δt	Time interval
ε_t/μ_t	Prices of natural gas/ electricity
β^{ET}/β^{SOFC}	Power cost of ET/ SOFC
β^{Li}/α^{Li}	Power/ capacity cost of li-ion battery
α^{HT}/V^{HT}	Capacity cost/volume of HT
$\xi_{j_3}^{Li.min}/\xi_{j_3}^{Li.max}$	Minimum/maximum charge status
w_m^{min}/w_m^{max}	Minimum/ maximum node pressure
ω_{max}	Max volume fraction of hydrogen
ϕ^{LD}/ϕ^{DER}	Volatility range of uncertainties
η^{P2G}/η^{P2G}	Conversion efficiency of P2G/G2P
c_{mn}/V^{HT}	Weymouth constant of the pipeline
C^G/C^E	Daily operating costs of GDN/ADN
C^{HGN}	Natural gas from HGN purchase costs
C^{P2G}	Purchase costs of gas from P2G
C^{G2P}/C^{TG}	Purchase costs of electricity from G2P/ upstream transmission grid
$C^{Li}/C^{SOFC}/C^{ET}/C^{HT}$	Usage costs of li-ion battery/ SOFC/ ET/ HT
HHV^{CH_4}/HHV^{H_2}	High heat value of CH ₄ / H ₂
$P_{j_1}^{ET}/P_{j_2}^{SOFC}/P_{j_3}^{Li}$	Rated power of ET/ SOFC/ li-ion battery
$E_{j_3}^{Li}$	Rated capacity of li-ion battery
$T^{ET}/T^{SOFC}/N_{j_3}^{Li}$	Lifetime of ET/SOFC/ li-ion battery
U_i^{min}/U_i^{max}	Min/max node voltage
r_{ij}/x_{ij}	Branch resistance/ reactance

D. Variables

ϑ_t^{P2G}	Price of power for P2G
ϑ_t^{G2P}	Price of gas for G2P
$P_{j_1,t}^{P2G}/P_{j_2,t}^{G2P}$	Power from P2G/G2P
$P_{j_3,t}^{Li.disc}/P_{j_3,t}^{Li.c}$	Li-ion battery discharge /charge power
$E_{j_3,t}^{Li}$	Li-ion battery store energy
$D_{j_3}/\xi_{j_3,t}^{Li}$	Li-ion battery charge depth/ charge status
$P_{j_4,t}^{DER}/Q_{j_4,t}^{DER}$	Active/reactive power injected by DER
P_t^{TG}	Electricity purchased from transmission grid
$P_{j,t}^{LD}/Q_{j,t}^{LD}$	Active/ reactive power load
$I_{i,j,t}/U_{i,t}$	Branch current/ Node voltage

> REPLACE THIS LINE WITH YOUR MANUSCRIPT ID NUMBER (DOUBLE-CLICK HERE TO EDIT) <

$P_{ij,t}/P_{jh,t}$	Active power flow
$Q_{ij,t}/Q_{jh,t}$	Reactive power flow
$G_{j_2,t}^{G2P}$	Volume of gas from G2P
$G_{n,t}$	Equivalent gas load volume
$G_{mn,t}/G_{ng,t}$	Branch gas flow
G_t^{HGN}	Natural gas purchased from HGN
$G_{n,t}^{H_2}/G_{n,t}^{LD}$	Volume of hydrogen injection / gas load
$G_{j_1,t}^{HT}$	Hydrogen volume stored in HT
$w_{m,t}/w_{n,t}$	Node pressure
HHV_t^{mix}	High heat value of gas mixture
$G_t^{CH_4}/G_t^{H_2}$	CH ₄ / H ₂ injected into the pipeline
ω_t	Volume fraction of hydrogen
$P_{j,t}^{LD.pre}/P_{j_4,t}^{DER.pre}$	Power load/ DER output forecast value
$P_{j,t}^{LD.real}/P_{j_4,t}^{DER.real}$	Power load/ DER output actual value
$P_{j_3,t}^{Li.pre}$	Power of li-ion battery in the first stage
$\Delta P_{j_3,t}^{Li}$	Power adjustment value of li-ion battery in the second stage

I. INTRODUCTION

To reduce dependence on fossil energy and also carbon emissions, distributed energy resources (DERs) are increasingly penetrating to ADN [1]- [2]. However, DER generation usually mismatch the load profiles due to its tremendous stochasticity, compromising DER utilization and stable ADN operation [3]. Regarding this issue, recent research proposes the formation of an IENGs by combining the ADN and GDN [4], which have emerged as flexible way to manage uncertain DERs and promote energy efficacy [5], drawing growing studies worldwide.

To further unleash the flexibility and efficiency of IENGs in [4]-[5], [6] proposes injecting hydrogen into the GDN to form a IENGs with the HCNG distribution network, and verifies the advantages of the proposed IENGs in local balancing of DERs and minimizing operational costs. Furthermore, the ‘‘GRHYD’’ project [7], invested by the French government, aims to inject green hydrogen into the existing GDN, and demonstrates the advantages of HCNG, including lower pollution levels and higher power generation efficiency. Additionally, compared to the gas turbines in the IENGs mentioned in [6], SOFCs have been demonstrated the better electrical efficiency and the wider fuel adaptability [8], [9]. Existing literature also revealed that, oriented to power grid steady operation applications, SOFC can be generically modelled following the gas turbine’s steady states [10]. Moreover, [11] validates the system stability of introducing SOFCs into ADN. Obviously, the above researches elucidate the feasibility and enormous development prospects of the HCNG-enabled IENGs bridged with SOFCs, however, there are still relatively little researches in related areas.

Upon the highly efficient infrastructure of HCNG-enabled GDN and SOFCs, profit pattern that advances development of the IENGs becomes another imminent issue. Previous research has established that, centrally controlled IENGs bespokes values in terms of stochasticity mitigation, renewable energy consumption, and social welfare increase [12]. More cognitions have manifested that centralized IENGs are away

from engineering, where GDN and ADN are usually operated by different independent entities. Even though these entities partially privatize their information, [13] proved that IENGs still benefits rich social welfare via the ADMM. In energy markets, in-depth problem for cooperative autonomous participants could come out, i.e., policy biases can render one stakeholder in weak position, and encumber the optimal social welfare [14]. Such policies can be, for example, economical penalties on renewable curtailment in power industries. Proper benefit sharing strategies are the key to solve the issue. The successes of Nash bargaining theory in other cooperative energy trading cases declare its salient merits on maximizing social benefits and fair benefit sharing [15]- [16]. However, its availability in the IENGs has not been investigated, let alone the concerned new IENGs, where GDN dominates the cooperation due to efficient HCNG-fueled SOFC and HCNG network.

Despite benefit sharing can facilitate stable operation of IENGs, profit collapse may still exist in the ADN side. Under the incentives of high-profit latency, SOFCs and HCNG network may participate more in ADN. Their slow responses force the ADN to buy costly electricity from upstream transmission grid to balance uncertainties of DERs [17], [18], triggering noticeable profit loss especially when there exists transactions bias due to over-prediction of DERs. [19] suggested configuring HESS to enhance rapid power balancing capability, and making look-ahead dispatch based on robust optimization to withstand slow-response hydrogen-to-power sources. Similar idea is also verified in [20], [21], where operational risks from uncertainties of renewable energy in traditional IENGs are mitigated by two-stage robust model. But the foregoing studies were not embarked on more complicated benefit sharing for standalone GDN and ADN. Furthermore, regarding the solution of the two-stage robust optimization issue, [22] inspired to use BCD algorithm to ease the intact two-stage model into tractable tri-level equivalence. The BCD is however uncorroborated in mastering decentralized multi-entity IENGs.

This paper brought forward configuration of multi-entity IENGs, benefit sharing mechanism to promote win-win collaboration, and tailored algorithm to dispatch the whole system.

The main contributions are three-fold:

(1) A promising IENGs model that bridges HCNG and electric distribution networks with SOFCs is proposed, where plethoric electricity produces hydrogen for HCNG, which is cyclically fed back to SOFCs to yield electricity. We show that such IENGs can benefit in more potentiality of cooperative earnings across the two heterogenous entity networks. Specifically, HCNG avoids hydrogen to methane, reducing energy dissipation by 17%, and SOFCs save 0.0412\$/kwh of energy conversion cost versus gas turbines.

(2) Strong policy-directed economical penalties on renewable curtailment render the ADN precarious in transactions with the GDN, easily inducing abnormally negative pricing (or even failed pricing) for electrolytic hydrogen from P2G. This undesired circumstance can be exacerbated when HCNG network with higher energy conversion efficiency collaborates with ADN. To solve this issue, a Nash bargaining-based bene-

> REPLACE THIS LINE WITH YOUR MANUSCRIPT ID NUMBER (DOUBLE-CLICK HERE TO EDIT) <

fit sharing mechanism is firstly proposed for HCNG-enabled GDN and ADN bridged by SOFCs. It is designed upon ADMM to ensure basic privacy for both entities, and can promote an enduring and stable win-win situation to actualize the latent profits from efficient energy conversion.

(3) For the first time, a two-stage robust Nash bargaining strategy with binding batteries is proposed towards more economical and stable ADN. The first stage places the proposed Nash bargaining, and the second stage leverages robust dispatch of li-ion batteries to promote economic operation of the ADN. Besides, a new ADMM and BCD joint algorithm bridged by C&CG is proposed to efficiently resolve the complex two-stage model, where the second stage of robust battery dispatch is turned into a tractable tri-level form and promptly solved via BCD, and is looped with the Nash bargaining by C&CG. Finally, the Appendix provides a proof of convergence for the algorithm mentioned above.

II. FRAMEWORK OF THE PROPOSED NCGN-ENABLED IENGs

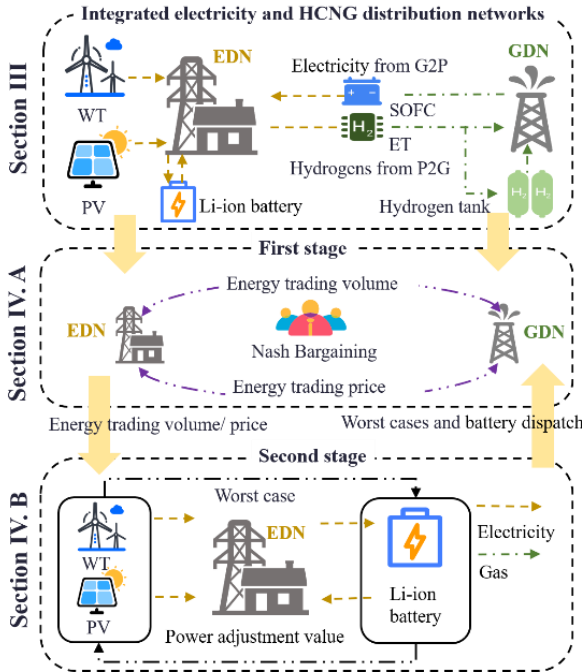


Fig. 1. The proposed two-stage robust benefit sharing framework.

Fig. 1 specifies the proposed two stage robust cooperative dispatch strategy for the two standalone entities of HCNG enabled GDN and ADN.

The first stage emulates the cooperative game between the two entities. Specifically, the transactions are carried out based on energy conversion infrastructures. The GDN is allowed to buy electricity from the ADN to yield hydrogen via ET, meanwhile the ADN can purchase HCNG from the GDN and generate power through HCNG-fueled SOFCs. To maximize social welfare and distribute benefits equally, Nash bargaining theory is adopted to settle the trading volume and prices in the designed transactions. The cooperative scheduling model and the benefit sharing strategy are depicted in section III and section IV. A, respectively.

The second stage takes in the trading volume as operational

baselines of energy conversion infrastructures, and conducts li-ion batteries to help the ADN alleviate the uncertainty by DERs. A designed subproblem is firstly employed to produce the worst operational cases under the given confidence intervals of DER power forecasts. Under these worst cases, dispatch for li-ion batteries is then settled to minimize purchasing electricity from upstream transmission grid and wipe out the transaction biases. After that, the li-ion battery dispatches and the produced worst cases are fed back to the first stage to correct the trading. The details of this stage are provided in section IV. B.

III. SCHEDULING MODEL OF INTEGRATED ELECTRICITY AND HCNG DISTRIBUTION NETWORKS

Following the designated NCGN-enabled IENGs, we settle the cooperative scheduling model for both utilities of HCNG-enabled GDN (i.e., the HCNG network) and ADN. Each entity works to increase its own profit, and is allowed to interact with the other entity via P2G or G2P equipment for more benefits. To improve energy conversion efficiency and promote latent social welfare, we bring in highly efficient P2G facility of HCNG-enabled SOFC, and a compact HCNG network that can bypass additional conversion from hydrogen to methane.

A. Scheduling Model of HCNG-enabled Network

The entity of the HCNG-enabled GDN intends to optimize its own yields, such that its own scheduling model will be set to maximize the income of selling gas to ADN, to minimize purchase cost of natural gas from HGN, purchase costs of hydrogen from P2G, and use costs of ET/HT, and to adhere to operational constraints of HCNG network, as given below:

$$\begin{aligned} & \min_{P_{j_1,t}^{P2G}, G_{j_2,t}^{G2P}, G_{j_1,t}^{HT}, \vartheta_t^{P2G}, \vartheta_t^{G2P}} C^G \quad (1) \\ \begin{cases} C^G = C^{HGN} + C^{P2G} + C^{ET} + C^{HT} - C^{G2P} \\ C^{HGN} = \sum_t \varepsilon_t G_t^{HGN} \\ C^{P2G} = \sum_j \sum_t \vartheta_t^{P2G} P_{j_1,t}^{P2G} \\ C^{ET} = \sum_{j_1} \sum_t \frac{\beta^{ET} P_{j_1,t}^{P2G} \Delta t}{P_{j_1}^{ET} \tau^{ET}} \\ C^{G2P} = \sum_{j_2} \sum_t \vartheta_t^{G2P} G_{j_2,t}^{G2P} \\ C^{HT} = \sum_{j_2} \frac{\alpha^{HT} V_{j_2}^{HT}}{\tau^{HT}} \end{cases} \quad (2) \end{aligned}$$

$$G_{n,t} = \sum_m G_{mn,t} + G_{n,t}^{H_2} + G_{n,t}^{HGN} - \sum_g G_{ng,t} + G_{n,t}^{H_2} \quad (3)$$

$$G_{j_1,t}^{H_2} = G_{j_2,t}^{G2P} - G_{j_1,t}^{HT}, G_{j_2,t}^{G2P} = \frac{\eta^{P2G} \cdot P_{j_1,t}^{P2G} \cdot \Delta t}{HHV^{H_2}} \quad (4)$$

$$G_{n,t} = (G_{n,t}^{LOAD} \cdot HHV^{CH_4}) / HHV_t^{mix} \quad (5)$$

$$\omega_t = G_t^{H_2} / (G_t^{H_2} + G_t^{CH_4}), \omega_t \leq \omega_{max} \quad (6)$$

$$HHV_t^{mix} = \omega_t HHV^{H_2} + (1 - \omega_t) HHV^{CH_4} \quad (7)$$

where the balance constraints of the gas network nodes are presented as (3)-(4). Changes in gas composition can affect the consumed volume [23], equivalent replacement of gas loads as shown in (5)-(7).

$$G_{mn,t} = \tau_{mn,t} \cdot c_{mn} \sqrt{\tau_{mn,t} (w_{m,t}^2 - w_{n,t}^2)} \quad (8)$$

$$\tau_{mn,t} = \begin{cases} 1 & w_{m,t} \geq w_{n,t} \\ -1 & w_{m,t} \leq w_{n,t} \end{cases} \quad (9)$$

> REPLACE THIS LINE WITH YOUR MANUSCRIPT ID NUMBER (DOUBLE-CLICK HERE TO EDIT) <

where the steady-state natural gas power flow constraints are formulated as (8)-(9) upon Weymouth equation. Considering that the GDN is radiant, the second-order cone relaxation can be used to convexify the constraints (8)-(9) into (10) [24].

$$\left\| \frac{G_{mn,t}}{c_{mn} w_{n,t}} \right\|_2 \leq c_{mn} w_{m,t}, w_{m,t}^{min} \leq w_{m,t} \leq w_{m,t}^{max} \quad (10)$$

To ensure that the second-order cone relaxation of natural gas power flow is exact, a penalty term on the nodal pressure difference is added to the objective function (11) [25].

$$\min_{P_{j_1,t}^{P2G}, G_{j_2,t}^{G2P}, C_{j_1,t}^{HES}, \theta_t^{P2G}, \theta_t^{G2P}} (C^G + \sum_t \sum_{m,n} \tau(w_{m,t} - w_{n,t})) \quad (11)$$

$$\forall t \in \mathbb{T}, j_1 \in \mathbb{J}_1, j_2 \in \mathbb{J}_2, m/n/g \in \mathbb{A}$$

B. Scheduling Model of Electric Distribution Network

The optimization goal of the ADN is to minimize daily operating costs in the worst scenarios, including purchase costs of electricity from upstream transmission grid, purchase costs of electricity from G2P units, and HESS usage costs, and to maximize incomes from the sale of P2G gas, as shown in (12)-(13).

$$\min_{P_{j_1,t}^{Li}, P_{j_1,t}^{P2G}, P_{j_2,t}^{G2P}, \theta_t^{P2G}, \theta_t^{G2P}} C^E \quad (12)$$

$$\begin{cases} C^E = C^{G2P} + C^{TG} + C^{HESS} - C^{P2G} \\ C^{TG} = \sum_t \mu_t P_t^{TG} \\ C^{HESS} = C^{Li} + C^{SOFC} \\ C^{Li} = \sum_{j_3} \frac{\sum_{t=1}^T ((\alpha^{Li} E_{j_3}^{Li} + \beta^{Li} P_{j_3}^{Li}) (P_{j_3,t}^{Li, disc} - P_{j_3,t}^{Li, c}) \cdot \Delta t)}{N_{j_3}^{Li} \cdot E_{j_3}^{Li} \cdot D_{j_3}} \\ N_{j_3}^{Li} = a_1 e^{(b_1 D_{j_3})} + a_2 e^{(b_2 D_{j_3})} \\ C^{SOFC} = \sum_{j_2} \sum_t \frac{\beta^{SOFC} P_{j_2,t}^{G2P} \Delta t}{P_{j_2}^{SOFC} \tau^{SOFC}} \end{cases} \quad (13)$$

where HESS usage costs consist of li-ion battery usage costs C^{Li} and SOFC usage costs C^{SOFC} . C^{Li} considers that depth of discharge (DOD) can affect the cycle life of li-ion battery [26], $N_{j_3}^{Li}$ is the number of cycles when the DOD is D_{j_3} , and a_1, a_2, b_1, b_2 are correlation coefficients

Distribution network power flow is formed as a standard second-order cone as in (14)-(15):

$$\hat{I}_{ij,t} = I_{ij,t}^2, \hat{U}_{i,t} = U_{i,t}^2 \quad (14)$$

$$\left\| \begin{array}{l} 2P_{ij,t} \\ 2Q_{ij,t} \end{array} \right\|_2 \leq \hat{I}_{ij,t} + \hat{U}_{i,t} \quad (15)$$

$$\left\| \hat{I}_{ij,t} - \hat{U}_{i,t} \right\|_2 \leq \hat{I}_{ij,t} + \hat{U}_{i,t} \quad (16)$$

$$(U_i^{min})^2 \leq \hat{U}_{i,t} \leq (U_i^{max})^2 \quad (16)$$

$$P_{j,t}^{LOAD} = \sum_i P_{ij,t} - r_{ij} \hat{I}_{ij,t} - \sum_h P_{jh,t} + P_{j,t}^{DER} + P_{j,t}^{G2P} + P_{j,t}^{Li} - P_{j,t}^{P2G} \quad (17)$$

$$P_{j_2,t}^{G2P} = G_{j_2,t}^{G2P} \cdot HHV_t^{mix} \cdot \eta^{G2P} \quad (18)$$

$$P_{j_3,t}^{Li} = P_{j_3,t}^{Li, pre} = P_{j_3,t}^{Li, disc} + P_{j_3,t}^{Li, c} \quad (19)$$

$$Q_{j,t}^{LOAD} = \sum_i Q_{ij,t} - x_{ij} \hat{I}_{ij,t} - \sum_h Q_{jh,t} + Q_{j,t}^{DER} \quad (20)$$

where (16)-(20) show the voltage security and power balance constraints for each bus in ADN.

$$E_{j_3,t}^{Li} = E_{j_3,t-1}^{Li} + \int_{t-1}^t P_{j_3,t}^{Li} \quad (21)$$

$$\xi_{j_3,t}^{Li} = E_{j_3,t}^{Li} / E_{j_3}^{Li}, \xi_{j_3,t}^{Li, min} \leq \xi_{j_3,t}^{Li} \leq \xi_{j_3,t}^{Li, max} \quad (22)$$

$$\begin{cases} -P_{j_3}^{Li} \leq P_{j_3,t}^{Li, c} \leq 0, 0 \leq P_{j_3,t}^{Li, disc} \leq P_{j_3}^{Li} \\ 0 \leq P_{j_2,t}^{G2P} \leq P_{j_2}^{SOFC}, 0 \leq P_{j_1,t}^{P2G} \leq P_{j_1}^{ET} \end{cases} \quad (23)$$

$$\forall t \in \mathbb{T}, j_1 \in \mathbb{J}_1, j_2 \in \mathbb{J}_2, j_3 \in \mathbb{J}_3, i, j, h \in \mathbb{B}$$

where (21)-(23) are the operational constraints of li-ion batteries, SOFCs, ETs.

IV. TWO-STAGE ROBUST NASH BARGAINING-BASED BENEFIT SHARING BETWEEN HCNG NETWORK AND ADN

To actualize the social welfare of the IENGs set on the HCNG network and the ADN, an all-win cooperation is imperative. Otherwise, ADN will be placed in a weak position, since it is stressed to consume RES, but HCNG network features requisite energy storage property to this end. To guarantee the benefits for the participating utilities, this section firstly introduces a privacy-preserving benefit sharing mechanism based on Nash bargaining theory and ADMM. On the other hand, motivated by the salient energy conversion efficiency of SOFCs and HCNG network, their foreseeable aggressive participation can jeopardize the ADN's ability to follow the shift of DER. Whereon, to de-risk reciprocity dis-equilibration between the two entities, a robust scheduling aided by li-ion batteries will be drawn into the whole cooperative model. Packed the above built models together via C&CG, we finally settle a two-stage robust Nash bargaining model aimed at stable social welfare.

A. Nash Bargaining between HCNG Network and ADN

The interaction between the GDN and the ADN is modelled using cooperative game, and the Pareto optimum between the two entities can be achieved fairly by constructing the following Nash bargaining model:

$$\begin{cases} \max_{P_{j_1,t}^{P2G}, P_{j_2,t}^{G2P}, \theta_t^{P2G}, \theta_t^{G2P}} (C_0^E - C^E)(C_0^G - C^G) \\ C^E \leq C_0^E, C^G \leq C_0^G \\ \text{s.t. (2)-(11), (13)-(23), } \forall t \in \mathbb{T}, j_1 \in \mathbb{J}_1, j_2 \in \mathbb{J}_2 \end{cases} \quad (24)$$

where C_0^E, C_0^G are the operating costs of ADN and GDN when they operate independently.

To solve the problem (24), we equivalently transform (24) into total benefit maximization problem (**Question 1**). The transaction price variables ($\{\theta_t^{P2G}, \theta_t^{G2P}\}$) in **Question 1** are eliminated, thus the volume of energy transaction ($\{P_{j_1,t}^{P2G}, G_{j_2,t}^{G2P}\}$) in **Question 1** can be directly solved to obtain the solution $[\check{P}_{j_1,t}^{P2G}, \check{G}_{j_2,t}^{G2P}]$.

Question 1:

$$\begin{cases} \max_{P_{j_1,t}^{P2G}, P_{j_2,t}^{G2P}} (C_0^E - C^{NET} - C^{HESS}) + (C_0^G - C^{HGN} - C^{ET}) \\ \text{s.t. (2)-(11), (13)-(23), } \forall t \in \mathbb{T}, j_1 \in \mathbb{J}_1, j_2 \in \mathbb{J}_2 \end{cases} \quad (25)$$

By converting (24) into logarithmic form, we obtain another equivalent optimization problem (**Question 2**).

Question 2:

$$\begin{cases} \max_{\theta_t^{P2G}, \theta_t^{G2P}} \ln(C_0^E - C^E) + \ln(C_0^G - C^G) \\ C^E \leq C_0^E, C^G \leq C_0^G \\ \text{s.t. (2)-(11), (13)-(23), } \forall t \in \mathbb{T} \end{cases} \quad (26)$$

where decision variables $[P_{j_1,t}^{P2G}, G_{j_2,t}^{G2P}]$ are replaced with fixed parameter $[\check{P}_{j_1,t}^{P2G}, \check{G}_{j_2,t}^{G2P}]$. Whereupon optimal energy transaction prices $[\check{\theta}_t^{P2G}, \check{\theta}_t^{G2P}]$ can be obtained by solving (26).

To ensure the privacy of the internal information of each

> REPLACE THIS LINE WITH YOUR MANUSCRIPT ID NUMBER (DOUBLE-CLICK HERE TO EDIT) <

entity, distributed optimization formulation (28)-(31) of (25)-(26) are built based on ADMM algorithm. Besides, to decouple $[P_{j_1,t}^{P2G}, G_{j_2,t}^{G2P}]$ and $[\vartheta_t^{P2G}, \vartheta_t^{G2P}]$, auxiliary variables are introduced in constraint (27) which needs to be enforced in the later.

$$\begin{cases} P_{j_1,t}^{P2GG} = P_{j_1,t}^{P2GP}, G_{j_2,t}^{G2PG} = G_{j_2,t}^{G2PP} \\ \vartheta_t^{P2GG} = \vartheta_t^{P2GP}, \vartheta_t^{G2PG} = \vartheta_t^{G2PP} \\ \forall t \in \mathbb{T}, j_1 \in \mathbb{J}_1, j_2 \in \mathbb{J}_2 \end{cases} \quad (27)$$

where $[P_{j_1,t}^{P2GG}, G_{j_2,t}^{G2PG}, \vartheta_t^{P2GG}, \vartheta_t^{G2PG}]$ represents the GDN's willingness to trade, $[P_{j_1,t}^{P2GP}, G_{j_2,t}^{G2PP}, \vartheta_t^{P2GP}, \vartheta_t^{G2PP}]$ represents the ADN's willingness to trade.

Question 1:

$$\begin{cases} \min L_1^E = C^{NET} + C^{HESS} - C_0^E + \\ \sum_{j_1} \sum_t \chi_{j_1,t}^P (P_{j_1,t}^{P2GG} - P_{j_1,t}^{P2GP}) + \frac{\rho_1}{2} (P_{j_1,t}^{P2GG} - P_{j_1,t}^{P2GP})^2 + \\ \sum_{j_2} \sum_t \chi_{j_2,t}^G (G_{j_2,t}^{G2PG} - G_{j_2,t}^{G2PP}) + \frac{\rho_2}{2} (G_{j_2,t}^{G2PG} - G_{j_2,t}^{G2PP})^2 \\ \text{s.t. (13)-(23), } \forall t \in \mathbb{T}, j_1 \in \mathbb{J}_1, j_2 \in \mathbb{J}_2 \end{cases} \quad (28)$$

$$\begin{cases} \min L_1^G = C^{GR} + C^{ET} - C_0^G + \\ \sum_{j_1} \sum_t \chi_{j_1,t}^P (P_{j_1,t}^{P2GG} - P_{j_1,t}^{P2GP}) + \frac{\rho_1}{2} (P_{j_1,t}^{P2GG} - P_{j_1,t}^{P2GP})^2 + \\ \sum_{j_2} \sum_t \chi_{j_2,t}^G (G_{j_2,t}^{G2PG} - G_{j_2,t}^{G2PP}) + \frac{\rho_2}{2} (G_{j_2,t}^{G2PG} - G_{j_2,t}^{G2PP})^2 \\ \text{s.t. (2)-(11), } \forall t \in \mathbb{T}, j_1 \in \mathbb{J}_1, j_2 \in \mathbb{J}_2 \end{cases} \quad (29)$$

Question 2:

$$\begin{cases} \min L_2^E = -\ln(C_0^E - C^E) + \\ \sum_t \gamma_t^P (\vartheta_t^{P2GG} - \vartheta_t^{P2GP}) + \frac{\rho_3}{2} (\vartheta_t^{P2GG} - \vartheta_t^{P2GP})^2 + \\ \sum_t \gamma_t^G (\vartheta_t^{G2PG} - \vartheta_t^{G2PP}) + \frac{\rho_4}{2} (\vartheta_t^{G2PG} - \vartheta_t^{G2PP})^2 \\ \text{s.t. (13)-(23), } \forall t \in \mathbb{T} \end{cases} \quad (30)$$

$$\begin{cases} \min L_2^G = -\ln(C_0^G - C^G) + \\ \sum_t \gamma_t^P (\vartheta_t^{P2GG} - \vartheta_t^{P2GP}) + \frac{\rho_3}{2} (\vartheta_t^{P2GG} - \vartheta_t^{P2GP})^2 + \\ \sum_t \gamma_t^G (\vartheta_t^{G2PG} - \vartheta_t^{G2PP}) + \frac{\rho_4}{2} (\vartheta_t^{G2PG} - \vartheta_t^{G2PP})^2 \\ \text{s.t. (2)-(11), } \forall t \in \mathbb{T} \end{cases} \quad (31)$$

where L_1^E, L_1^G (L_2^E, L_2^G) are the augmented Lagrangian functions for the ADN and GDN about **Question 1** (**Question 2**). $\chi_{j_1,t}^P, \chi_{j_2,t}^G, \gamma_t^P, \gamma_t^G, \rho_1, \rho_2, \rho_3, \rho_4$ are the Lagrangian multipliers.

In summary, the Nash bargaining process mentioned above can be understood as the social benefits obtained through jointly maximizing and then fairly sharing the social benefits. If any party submits false transaction information, it will cause the derived trading strategy to deviate from the solution that maximizes social welfare, ultimately reducing the distributed benefits [27]. Therefore, ADN and GDN have no motivation to falsely report transaction information, which is in line with incentive compatibility.

B. Two-stage Robust Nash Bargaining Involving Li-ion Battery and Its Solving Scheme

Taking account of uncertainties, the ADN is at risk of failing to achieve the desired effect of prior trading decisions, therefore, a two-stage robust model is established, as shown in (32)-(33), where $\mathbf{y} = [P_{j_3,t}^{Li.pre}, P_{j_1,t}^{P2G}, P_{j_2,t}^{G2P}, \vartheta_t^{P2G}, \vartheta_t^{G2P}]$ is the first stage decision variable, $\mathbf{x} = [\Delta P_{j_3,t}^{Li}]$, is the second stage decision variable, $\mathbf{u} = [P_{j_3,t}^{Li.real}, P_{j_4,t}^{DER.real}]$. is the worst case of uncertain variable. Besides, based on constraints (13)-(23),

the constraints of uncertain variables are added to (33).

$$\begin{aligned} & \min_{\mathbf{y}} \max_{\mathbf{u}} \min_{\mathbf{x}} C^E \quad (32) \\ & \text{s.t. (13)-(23)} \\ & \begin{cases} P_{j_3,t}^{Li} = P_{j_3,t}^{Li.pre} + \Delta P_{j_3,t}^{Li} = P_{j_3,t}^{Li.disc} + P_{j_3,t}^{Li.c} \\ 0 \leq (P_{j_3,t}^{LOAD.real} - P_{j_3,t}^{LOAD.pre}) / P_{j_3,t}^{LOAD.pre} \leq \phi^{LOAD} \\ 0 \leq (P_{j_4,t}^{DER.real} - P_{j_4,t}^{DER.pre}) / P_{j_4,t}^{DER.pre} \leq \phi^{DER} \\ 0 \leq P_{j_4,t}^{DER} \leq P_{j_4,t}^{DER.real}, P_{j_3,t}^{LOAD} = P_{j_3,t}^{LOAD.real} \end{cases} \quad (33) \\ & \forall t \in \mathbb{T}, j_1 \in \mathbb{J}_1, j_2 \in \mathbb{J}_2, j_3 \in \mathbb{J}_3, j_4 \in \mathbb{J}_4, j \in \mathbb{B} \end{aligned}$$

Through C&CG algorithm, the two-stage robust model is decomposed into the main problem (MP) and the subproblem (SP). As shown in Fig. 2, the MP serves to optimize the volume and prices of the energy transaction, through the model presented in section IV. A. The sub-problem is responsible for figuring out the worst cases of random variables, and planning the power adjustment profiles of li-ion batteries to de-risk profit collapse due to stochastic nature of DERs. Additionally, the detailed proof of the convergence of the algorithm proposed can be found in the Appendix.

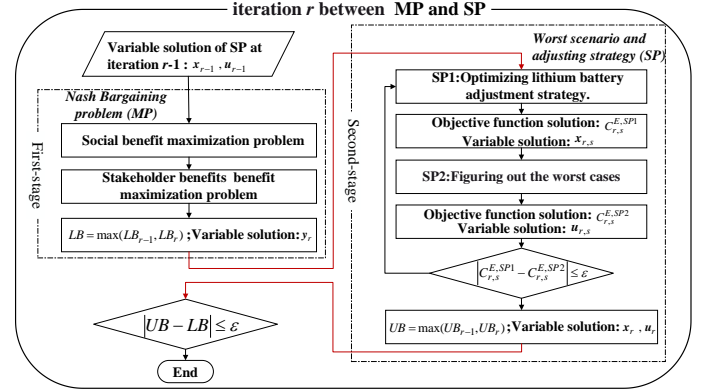


Fig. 2. Solving scheme of the proposed two-stage robust benefit sharing model between HCNG-enabled GDN and ADN

The MP and SP at iteration r of the C&CG algorithm is formulated as (34)-(35).

$$\text{MP: } \begin{cases} C_r^{E,SP} = \min_{\mathbf{y}} C^E \\ \text{(28)-(31)} \\ \mathbf{x} = \check{\mathbf{x}}_{r-1}, \mathbf{u} = \check{\mathbf{u}}_{r-1} \end{cases} \quad (34)$$

$$\text{SP: } \begin{cases} C_r^{E,SP} = \max_{\mathbf{u}} \min_{\mathbf{x}} C^E \\ \mathbf{y} = \check{\mathbf{y}}_r \\ \text{s.t. (13)-(23)} \end{cases} \quad (35)$$

where $\check{\mathbf{x}}_{r-1}, \check{\mathbf{u}}_{r-1}$ are solutions of decision variable in the second stage and the worst case of SP, respectively, at iteration $r-1$, which will be set to a cutting plane constraints of MP. $\check{\mathbf{y}}_r$ is decision variable of MP solved in the first stage, at iteration r , which will be set to cutting plane constraints of SP. In this regard, MP and SP become a two-level solving loop.

Since the SP is a max-min problem and cannot be solved directly, to solve it, the BCD algorithm is used to decompose the SP into two tractable problems of subproblem1 (SP1) and subproblem2 (SP2). Note that, SP1 and SP2 construct an inner loop of their upstream solving loop of MP-SP.

In the at s th iteration of SP1-SP2 inner solving loop, the

> REPLACE THIS LINE WITH YOUR MANUSCRIPT ID NUMBER (DOUBLE-CLICK HERE TO EDIT) <

BCD algorithm sequentially solves (36) and (37).

$$\text{SP1: } \begin{cases} C_{r,s}^{E,SP1} = \min_x C^E \\ \mathbf{y} = \check{\mathbf{y}}_r, \mathbf{u} = \check{\mathbf{u}}_{r,s-1} \\ \text{s.t. (13)-(23)} \end{cases} \quad (36)$$

where the random variables \mathbf{u} are fixed as $\check{\mathbf{u}}_{r,s-1}$, which is the worst case of SP2 at iteration $s-1$, during the r th solving loop of MP and SP.

$$\text{SP2: } \begin{cases} C_{r,s}^{E,SP2} = \max_u C^E \\ \mathbf{y} = \check{\mathbf{y}}_r, \mathbf{x} = \check{\mathbf{x}}_{r,s} \\ \text{s.t. (13)-(23), } \forall t \in \mathbb{T}, j_4 \in \mathbb{J}_4, j \in \mathbb{B} \end{cases} \quad (37)$$

where \mathbf{x} is fixed as $\check{\mathbf{x}}_{r,s}$, which is the optimal decision variable of SP1 at iteration s .

C. Convergence Proof of the Proposed Solving Algorithm

To solve the proposed two-stage robust benefit sharing model between HCNG-enabled GDN and ADN, a new ADMM and BCD joint algorithm bridged by C&CG is proposed in this paper. The following theorem establishes the convergence for the ADMM and BCD joint algorithm bridged by C&CG.

Theorem 1: The proposed algorithm should satisfy the following three conditions for convergence:

- 1) Objective function C^E and C^G in MP are closed and convex.
- 2) Objective function C^E in SP is continuously differentiable and convex
- 3) Feasible region of variable \mathbf{u} is a bounded closed set.

Proof. Please see Appendix.

V. NUMERICAL STUDIES

A IENGs consisting of an IEEE 33-bus ADN and a 20-node Belgian GDN is studied, as shown in Fig.3, where solar and wind power generation data are from Elia, power and gas load data are collected from [28]. In IEEE 33-bus ADN, DERs are integrated at bus E17, E21, E24, and E32, bus E17 and E32 own li-ion batteries, bus E6 and E12 are connected to node G8 and G4 of the GDN through SOFCs. Voltage limits of all power buses are within [0.95, 1.05] p.u. The uncertainties of DER generation and load are simulated via 15% and 5% intervals upon their forecasting baselines. In 20-node GDN, HT is integrated at node G0, and two ETs are set on node E17 and E24.

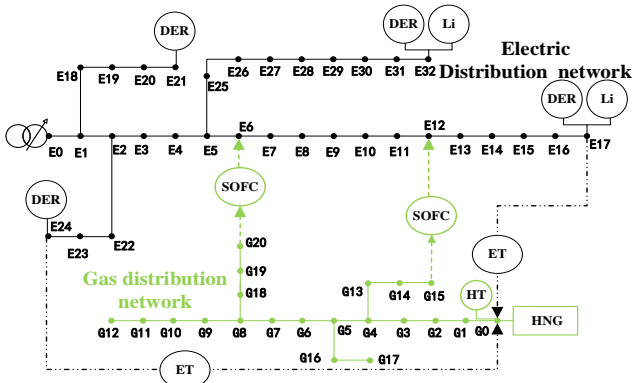


Fig. 3. Configuration diagram of combined optimization model between electricity and HCNG distribution networks.

A. Efficiency analysis of cooperative ADN and GDN

To prove the effectiveness of the proposed cooperative operational framework, three competitive models are given:

Model 1: The proposed cooperative ADN and GDN.

Model 2: No cooperation between ADN and GDN. Following [29], ADN configures its own li-ion batteries, HT and SOFCs, and goes self-energy conversion between electricity and hydrogen. The **Model 2** can be deemed as a development of the architecture in [30], and it can help figure out if SOFCs can turn this self-energy conversion loop to be profitable.

Model 3: No cooperation between ADN and GDN, and only li-ion batteries are included in ADN [31]. This is a common case known as active distribution network. The **Model 3** come out to highlight the high capacity and cost-effectiveness merits of the proposed IENGs architecture.

Without uncertainty involved, the daily operating costs, energy conversion loss rate, and the marginal cost of ET and SOFC (i.e., the sensitivity of their cost versus the produced energy) are shown in Tab. I. Benefit ingredients and energy conversion profiles are shown in Tab. II and Fig. 4.

TABLE I
DAILY OPERATING COSTS WITHOUT UNCERTAINTY CONSIDERED

Model #	Operating Costs \$	Energy Conversion Loss Rate	Marginal cost \$/kWh
Model 1	ADN 1537	27%	0.0307
	GDN 23614		
Model 2	ADN 1699	44%	0.0719
	GDN 23809		
Model 3	ADN 1755	-	-
	GDN 23809		

TABLE II
INGREDIENTS ANALYSIS OF COST AND BENEFIT (\$)

Model	Benefit*	C^{SOFC}	C^{ET}	C^{TG}	C^{HGN}
Model 1	ADN 218	273	116	240	24220
	GDN 194				
Model 2	ADN 56	27	34	1271	23809

*Benefits of ADN and GDN are calculated via $C_0^E - C^E$ and $C_0^G - C^G$, respectively.

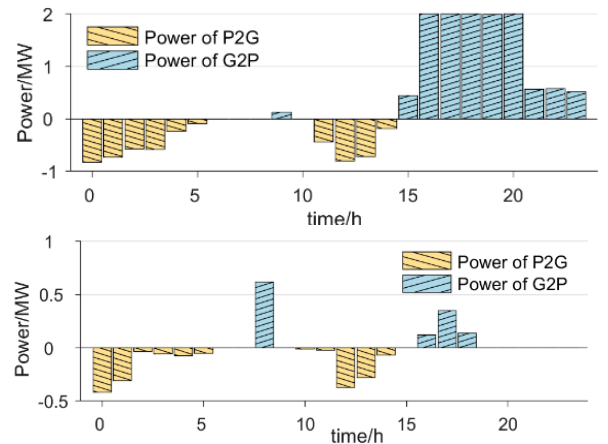


Fig. 4. Energy conversion profiles. Note that, positive power indicates that the energy conversion runs from gas to power, also the power injection to the ADN (top: **Model 1**, bottom: **Model 2**).

From Tab. I and Tab. II, daily operating cost of ADN by **Model 1** is similar to that by **Model 2**, both reducing the ADN's cost by nearly 12% against **Model 3**. However, **Model 1** significantly outperform **Model 2** regarding daily operating

> REPLACE THIS LINE WITH YOUR MANUSCRIPT ID NUMBER (DOUBLE-CLICK HERE TO EDIT) <

costs of GDN. **Model 1** creates the best social welfare which is nearly 1.6% to total cost, while guaranteeing ADN benefits. In **Model 1**, the ADN gets profits by either selling hydrogen or buying HCNG to generate electricity below the time-of-use electricity price, and GDN earns by two paths of selling natural gas and yielding low-priced hydrogen. Whereas, in **Model 2**, ADN can only gain from the price gap between the low-priced local renewable energies and the high-priced electricity of upstream grid. Besides, **Model 2** only allows conversion between pure hydrogen and power, without off-the-shelf fuel supplement from GDN, it thus results in an enormous energy loss rate of 44%, and is beat by **Model 1** in term of energy conversion's marginal cost (i.e., 0.0719 \$/kWh vs. 0.0307 \$/kWh), which implies the waste of energy and the decline in social welfares.

In addition, from Fig. 4, **Model 1** successfully distributes the yielded benefits to ADN and GDN through the Nash bargaining model. This demonstrates the feasibility of the proposed benefit sharing strategy.

B. Verification of the proposed robust benefit sharing strategy

Robust benefit sharing de-risks profit collapse due to forecasting error. Here we consider three robust cases (**Case 2~Case 4**). Notably, **Case 1** is a deterministic case that assumes forecasts are exact, which in fact corresponds to single MP.

Case 1: The forecasts of load and DERs generation are exact.

Case 2: The forecast of DER generation is exact, while load profile is produced by the robust optimization procedure SP2.

Case 3: The forecast of load is exact, DER generation profile is produced by the robust optimization procedure SP2.

Case 4: Load and DERs generation profiles are both produced by the robust optimization procedure SP2.

Case 2~Case 4 establish the testing robust operational set. To show the importance of li-ion batteries in robust benefit sharing, daily operating costs with or without lithium battery power redispatch as shown in Tab. III.

TABLE III
OPERATING COSTS WITH OR WITHOUT LI-ION BATTERY POWER REDISPATCH (\$)

Entities	Case 1	Case 2		Case 3		Case 4	
		No bat.	With bat.	No bat.	With bat.	No bat.	With bat.
ADN	1537	2017	1922	3038	2859	3636	3459
GDN	23614	23614	23614	23614	23614	23614	23614

From Tab. III, two results can be found. The one is a trivial conclusion, which indicates that operating costs increase along with consideration of robustness. On the other hand, under **Case 2~Case 4**, li-ion batteries help improve operational economic by nearly 5.5% on average. The reason is that, the slow responses of SOFCs and ETs cannot balance the power drift of stochastic variables (DER generation and load) in real-time, so the ADN can only conduct either fast power regulation equipment or buy electricity from upstream transmission grid towards power balance. By li-ion batteries, the costly electricity purchase from transmission grid can be reduced, even though lifetime operational costs are embraced in dispatch.

We further study how the robust benefit sharing help mitigate profit collapse for the ADN, and Tab. IV is whereupon provided below. Since forecasting error of load and DER generation exists, there must be power imbalances in intraday operations. Towards power balance, whether the ADN pays auxiliary service fees to li-ion batteries or purchases electricity from upstream transmission grid, its profit collapse always comes from the transaction bias between the day-ahead cooperative IENGs schedule and intraday true operations of load and DERs. So, a trivial assumption that only considers electricity purchase from upstream power grid is made during the forming of Tab. IV.

TABLE IV
IMPLEMENTATION COSTS OF DAY-AHEAD SCHEDULES ON INTRADAY CASES (\$)

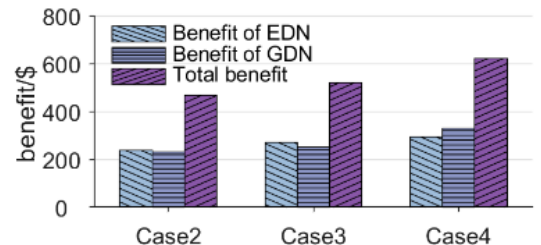
Testing intraday operational case/set	Proposed Robust benefit sharing (with SP)		Deterministic benefit sharing (excluding SP)	
	C^E	C^{TG}	C^E	C^{TG}
Case 1	1537	240	1537	240
Case 2	1906	399	1922	857
Case 3	2551	776	2859	1919
Case 4	3089	1250	3459	2519
Mean±var. stat. under robust set	2271±595	666±389	2444±758	1309±892

In. Tab. IV, there is clear trends of decreasing operating cost of the ADN (C^E) by the proposed method. Also, more uncertainties enlarge the risk of profit collapse, as you can see **Case 4** manifests the largest increase of cost in the comparison between our method and the deterministic one. The cost statistics revealed that, the robust strategy indeed stabilizes the profit of the ADN to withstand forecasting errors of uncertainties, and its decision pattern is to facilitate interactions between the ADN and the GDN to reduce costly electricity purchase from upstream power grid (C^{TG}), which will be further analyzed later.

To further justify the proposed framework, Tab. V, Fig. 5, Fig. 6, and Fig. 7 are provided. These outcomes stem from comparative experiments under the given robust operating cases.

TABLE V
TOTAL OPERATING COSTS BY COMPETITIVE MODELS IN DIFFERENT ROBUST CASES (\$)

Case #	Entities	Model 1	Model 2	Model 3
Case 2	ADN	1906	2011	2143
	GDN	23579	23809	23809
Case 3	ADN	2551	2816	2820
	GDN	23558	23809	23809
Case 4	ADN	3089	3382	3382
	GDN	23480	23809	23809



> REPLACE THIS LINE WITH YOUR MANUSCRIPT ID NUMBER (DOUBLE-CLICK HERE TO EDIT) <

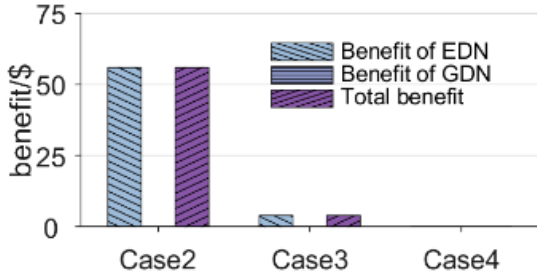


Fig. 5. Benefit analysis (Top: Model 1. Bottom: Model 2).

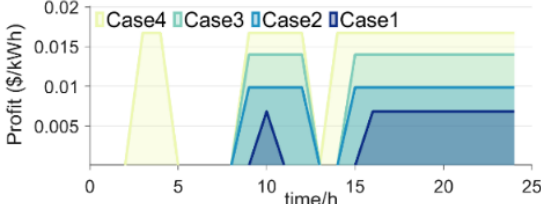
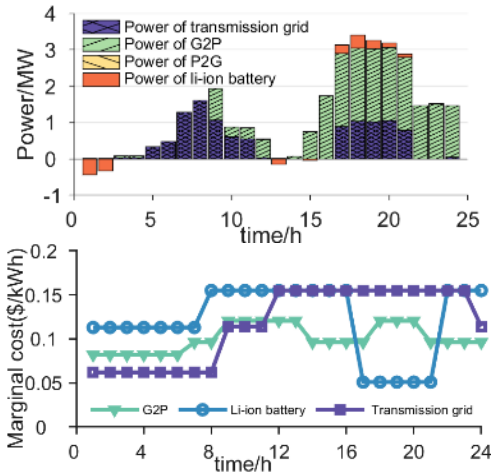
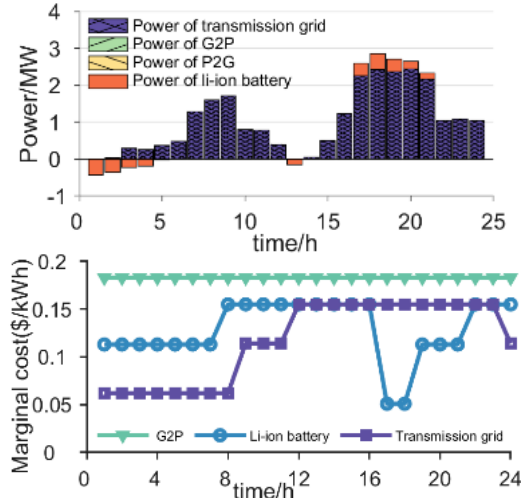


Fig. 6. Marginal profit of the GDN selling HCNG upon the proposed benefit sharing mechanism (Model 1) under the testing robust cases.

Tab. V and Fig. 5 present the best cost-benefit stability of the proposed method compared to other rivals. Illustrative data are the dramatically decreasing benefit by Model 2 from Case 2 to Case 3, as shown in the bottom subplot of Fig. 5. Relatively, our method gains stable benefits for both ADN and GDN, no matter what extreme cases happen. Besides, it is apparent that, Model 1 results in the best economy of GDN, as GDN can gain extra benefits by energy conversion with ADN. We can further explain the above conditions by means of Fig. 6. In Fig. 6, marginal profit of the GDN selling HCNG increases from Case 1 to the worst Case 4. The worse operating cases of the ADN incent more sale of HCNG fuel from the GDN, such that the GDN earns more. The incomes will then be shared to the ADN to contribute to a risk-averse and stable benefits for both entities. In this win-win situation, GDN gains extra payback and help stabilize the operation of ADN to consolidate ongoing gains. Yet, this is not the case for Model 2, since in contrast to the tremendous gas storage of the GDN, the storage capacity of self-hydrogen and electricity conversion is negligible and of high use expense, hydrogen storage cannot be benefited.



(a) Model 1



(b) Model 2

Fig. 7. Profiles of operations and marginal costs of involved infrastructures under Case 4.

Fig. 7 interprets the significance of the SOFC-bridged cooperative mechanism between the ADN and the HCNG-enabled GDN. As shown in Fig. 7, during 15~24 h where DER generation plummet, G2P transactions in the framework of Model 1 are prolifically stimulated, because of two origins. On one hand, upon our designed IENGs, marginal cost of HCNG-to-power is stable and regulated much lower than that of electricity from upstream grid. On the other hand, although li-ion batteries hold the best marginal cost, they lack controllable capacity to serve as critical flexible resources in such extreme Case 4, whereas GDN's storage capacity is immense. Regarding Model 2, self-hydrogen storage manifests the largest marginal cost, thus the ADN would rather adopt electricity from upstream power grid than hydrogen storage. However, the former is noticeably costly than the applied HCNG-to-power (by over 20%), wherefore the proposed Model 1 is more lucrative for growth.

VI. CONCLUSION

This paper proposes a two-stage robust Nash bargaining-based benefit sharing mechanism to facilitate stable cooperation between HCNG network and electric distribution network, that are bridged with SOFCs. To effectuate the latent social welfare implied in the efficient energy conversion of HCNG-enabled SOFCs, a stable cooperation framework is firstly proposed based on Nash bargaining. Then, a robust Nash bargaining that incorporates li-ion batteries is proposed to de-risk the ADN's profit collapse from transaction bias. We finally design a two-stage solving strategy to master the proposed model, where the first stage ensures privacy of the two utilities via ADMM, the second stage efficiently dispatches li-ion batteries to withstand the worst operational cases of ADN via emerging BCD algorithm, and the two stages are looped upon C&CG. Numerical study shows that the proposed scheme circumvents profit collapse, fulfills stable gains for both HCNG network and ADN, and reaches a stable social welfare of nearly 1.6% to total cost.

> REPLACE THIS LINE WITH YOUR MANUSCRIPT ID NUMBER (DOUBLE-CLICK HERE TO EDIT) <

APPENDIX

The proof of **Theorem 1** consists of three main parts, as detailed below:

A. The convergence of ADMM for MP

Lemma 1. [32]: The ADMM algorithm solves problems in the form: $\min f(x) + g(x)$, if the (extended-real-valued) functions $f: \mathbb{R}^n \rightarrow \mathbb{R} \cup \{+\infty\}$ and $g: \mathbb{R}^m \rightarrow \mathbb{R} \cup \{+\infty\}$ are closed and convex, ADMM algorithm is converge.

Proof. In section IV(A), Nash bargaining model is transformed into **Question 1** and **Question 2**. The transaction price variables ($\{\vartheta_t^{P2G}, \vartheta_t^{G2P}\}$) in **Question 1** are eliminated, thus, the objective function in (25) and (28)- (29) are linear functions about variables: $\{P_{j_1,t}^{P2G}, G_{j_2,t}^{G2P}, G_{j_1,t}^{HT}, P_{j_3,t}^{Li}, P_{j_1,t}^{P2G}, P_{j_2,t}^{G2P}\}$, where the objective function in (25) and (28)- (29) can be considered $\min f(x) + g(x)$, f and g in Lemma 1. Therefore, the objective functions and the feasible region in (28)- (29) are convex and closed obviously and ADMM is converge in **Question 1**.

In **Question 2** energy transaction variables ($\{P_{j_1,t}^{P2G}, G_{j_2,t}^{G2P}\}$) multiplied by transaction price variables ($\{\vartheta_t^{P2G}, \vartheta_t^{G2P}\}$) are replaced with fixed parameter $[\check{P}_{j_1,t}^{P2G}, \check{G}_{j_2,t}^{G2P}]$. Thus, the objective function about variables $\{\vartheta_t^{P2G}, \vartheta_t^{G2P}\}$ in (26) and (30)-(31) are also convex. The next proof of ADMM's convergence in **Question 2** is same as **Question 1**. Due to the convergence of **Question 1** and **Question 2**, MP also converges. \square

B. The convergence of BCD for SP

Lemma 2. [33]: If the function f in problem $\min f(\mathbf{x}): \mathbf{x} \in \mathbb{R}^n$ is continuously differentiable and convex, the optimal solution of function $\arg \min_{\mathbf{x} \in \mathbb{R}^n} f(x_1, \dots, x_{i-1}, x_i, x_{i+1}, \dots, x_m)$ is unique and the BCD algorithm is converge.

Proof. In section IV(B), the variables ($\mathbf{y} = [P_{j_3,t}^{Li,pre}, P_{j_1,t}^{P2G}, P_{j_2,t}^{G2P}, \vartheta_t^{P2G}, \vartheta_t^{G2P}]$) in SP(35) is replaced with fixed parameter $\check{\mathbf{y}}_r$, thus, the objective function (C^E) of (35) is a linear function, which is continuously differentiable and convex obviously. Therefore, the SP satisfies the convergence condition of Lemma 2. \square

C. The convergence of the proposed ADMM and BCD joint algorithm bridged by C&CG

To start our proof, we firstly introduce a necessary lemma regarding the convergence of the C&CG algorithm:

Lemma 3. [34-35]: The C&CG algorithm decomposes the original problem into main problems and sub-problems that iteratively interact with each other, and two sequences of upper and lower bounds of original problem $\{UB^t\}$, $\{LB^t\}$ are obtained during the process of algorithm iteration. If there exist two non-empty and bounded sequences $\{UB^t\}$, $\{LB^t\}$ such that $|UB^t - LB^t| \rightarrow 0$, C&CG algorithm will terminate in a finite number of iterations, then the C&CG algorithm is converge.

Proof. The optimal solution of the two-stage robust optimization is the objective value in the worst-case scenario, in other words, the optimal decision holds for all values of uncer-

tainty scenarios (\mathbf{u}). The cutting planes added in the master problem only optimize under partial uncertainty scenarios, thus, MP (34) is a relaxation problem of original problem (32), and since it seeks to minimize C^E , $C_r^{E,MP}$ is definitely a lower bound for the original problem (32).

In addition, in SP (35), \mathbf{y} is fixed to a constant value $\check{\mathbf{y}}_r$ from (34), which is not necessarily the optimal solution of original problem (32). Therefore, $C_r^{E,SP}$ is a feasible solution of original problem (32), which is greater than or equal to the optimal solution, $C_r^{E,SP}$ is definitely a upper bound for the original problem (32).

In the aforementioned iteration process, both MP (34) and SP (35) search for the maximum or minimum value of C^E within the feasible domain along the gradient, and obtain two sequences of upper and lower bounds ($C_r^{E,SP} \in \mathbf{UB}$ and $C_r^{E,MP} \in \mathbf{LB}$).

In the function C^E of SP2 (37), $[\mathbf{y}, \mathbf{x}]$ are fixed as constants $[\check{\mathbf{y}}_r, \check{\mathbf{x}}_{r,s}]$, thus, only C^{TG} include variables:

$$C^{TG} = \sum_t \mu_t P_t^{TG} \quad (A1)$$

$$P_t^{TG} = \sum_j (P_{j,t}^{LOAD} - P_{j,t}^{DER} - P_{j,t}^{G2P} - P_{j,t}^{Li} + P_{j,t}^{P2G}) \quad (A2)$$

where $[P_{j,t}^{G2P}, P_{j,t}^{Li}, P_{j,t}^{P2G}] \in [\mathbf{y}, \mathbf{x}]$ are fixed as constants, $P_{j,t}^{DER}$ and $P_{j,t}^{LOAD}$ are variables.

$$0 \leq P_{j_4,t}^{DER} \leq P_{j_4,t}^{DER,real}, P_{j_4,t}^{LOAD} = P_{j_4,t}^{LOAD,real} \quad (A3)$$

Taking into account the inequality constraint relationship between variable $P_{j_4,t}^{DER,real} \in \mathbf{u}$ and variable $P_{j_4,t}^{DER}$ in the objective function C^E , a set of variables κ are introduced and $\forall \kappa_{j_4,t} \in \kappa$ satisfies the constraint of (A3):

$$\begin{cases} \kappa_{j_4,t} + P_{j_4,t}^{DER} = P_{j_4,t}^{DER,real} \\ \kappa_{j_4,t}^{min} \leq \kappa_{j_4,t} \leq \kappa_{j_4,t}^{max} \end{cases} \quad (A4)$$

Based on the above deduction, the first-order Taylor expansion formula for variable $\mathbf{u} = [P_{j,t}^{LD,real}, P_{j_4,t}^{DER,real}]$ at point $\check{\mathbf{u}}_{r,s-1} = [\check{P}_{j,t,r,s-1}^{LOAD}, \check{P}_{j_4,t,r,s-1}^{DER}]$ in the function C^E of (36) is:

$$F(\mathbf{u}) = C_{r,s-1}^{E,SP2} + \sum_t \sum_j \mu_t (P_{j,t}^{LOAD,real} - \check{P}_{j,t,r,s-1}^{LOAD}) + \sum_t \sum_{j_4} (\mu_t (\kappa_{j_4,t} - \check{\kappa}_{j_4,t,r,s-1}) - \mu_t (P_{j_4,t}^{DER,real} - \check{P}_{j_4,t,r,s-1}^{DER})) \quad (A5)$$

In order to maximize the value of C^E , the variable $\kappa_{j_4,t} / P_{j_4,t}^{LOAD,real}$ tends to approach the maximum value $\kappa_{j_4,t}^{max} / P_{j_4,t}^{LOAD,max}$ within its range, the variable $P_{j_4,t}^{DER,real}$ tends to approach the maximum value $P_{j_4,t}^{DER,min}$ within its range. If the number of iterations between SP1 and SP2 tends to infinity ($s \rightarrow \infty$), the target solution $C_r^{E,SP}$ and variable solution $\check{\mathbf{u}}_r$ are obtained, and if the number of iterations between MP and SP tends to infinity ($r \rightarrow \infty$), $\kappa_{j_4,t} / P_{j_4,t}^{LOAD,real} / P_{j_4,t}^{DER,real}$ will converge to $a_\kappa / a_{load} / a_{DER}$ ($a_\kappa \leq \kappa_{j_4,t}^{max}$, $a_{load} \leq P_{j_4,t}^{LOAD,max}$, $a_{DER} \leq P_{j_4,t}^{DER,real}$), then, $|\check{\mathbf{u}}_r - \check{\mathbf{u}}_{r-1}| \rightarrow 0$.

The optimal values of both the first-stage and second-stage variables $[\mathbf{y}, \mathbf{x}]$ change due to variations in the scenario variables \mathbf{u} . If $|\check{\mathbf{u}}_r - \check{\mathbf{u}}_{r-1}| \rightarrow 0$, variables \mathbf{y} and \mathbf{x} will trend towards convergence as well, then, $|C_r^{E,SP} - C_{r-1}^{E,MP}| \rightarrow 0$.

Finally, based on the proof in Appendix A and , MP and SP converge separately. Furthermore, because the feasible region of variable \mathbf{u} is bounded and closed, the number of iterations r between the main problem and the subproblem is finite. Thus, there must exist two bounded sequences (\mathbf{UB} and \mathbf{LB}) for that

> REPLACE THIS LINE WITH YOUR MANUSCRIPT ID NUMBER (DOUBLE-CLICK HERE TO EDIT) <

make the proposed ADMM and BCD joint algorithm bridged by C&CG converge in a finite number of iterations. □

REFERENCES

- [1] International Renewable Energy Agency, "Global energy transformation: A roadmap to 2050," Abu Dhabi, UAE, 2019, Accessed: Jun. 17, 2021. [Online]. Available: <https://www.irena.org/publications>.
- [2] M. Fan, K. Sun, D. Lane, W. Gu, Z. Li, and F. Zhang, "A Novel Generation Rescheduling Algorithm to Improve Power System Reliability With High Renewable Energy Penetration," *IEEE Trans. Power Syst.*, vol. 33, no. 3, pp. 3349–3357, May 2018.
- [3] J. Duan, F. Liu, and Y. Yang, "Optimal operation for integrated electricity and natural gas systems considering demand response uncertainties," *Applied Energy*, vol. 323, p. 119455, Oct. 2022.
- [4] G. Fambri, C. Diaz-Londono, A. Mazza, M. Badami, T. Sihvonen, and R. Weiss, "Techno-economic analysis of Power-to-Gas plants in a gas and electricity distribution network system with high renewable energy penetration," *Applied Energy*, vol. 312, p. 118743, Apr. 2022.
- [5] J. Duan, Y. Yang, and F. Liu, "Distributed optimization of integrated electricity-natural gas distribution networks considering wind power uncertainties," *Int. J. Electr. Power Energy Syst.*, vol. 135, p. 107460, Feb. 2022.
- [6] C. Fu, J. Lin, Y. Song, J. Li, and J. Song, "Optimal Operation of an Integrated Energy System Incorporated With HCNG Distribution Networks," *IEEE Trans. Sustain. Energy*, vol. 11, no. 4, pp. 2141–2151, Oct. 2020.
- [7] ENGIE, "The GRHYD demonstration project," [Online]. Available: <https://www.engie.com/en/businesses/gas/hydrogen/power-to-gas/the-grhyd-demonstration-project>.
- [8] H. Chen, C. Yang, N. Zhou, N. Farida Harun, D. Oryshchyn, and D. Tucker, "High efficiencies with low fuel utilization and thermally integrated fuel reforming in a hybrid solid oxide fuel cell gas turbine system," *Applied Energy*, vol. 272, p. 115160, Aug. 2020.
- [9] A. S. Mehr, A. Moharramian, S. Hossainpour, and D. A. Pavlov, "Effect of blending hydrogen to biogas fuel driven from anaerobic digestion of wastewater on the performance of a solid oxide fuel cell system," *Energy*, vol. 202, p. 117668, Jul. 2020.
- [10] Q. Hou, H. Zhao, and X. Yang, "Economic performance study of the integrated MR-SOFC-CCHP system," *Energy*, vol. 166, pp. 236–245, Jan. 2019.
- [11] F. Jurado, M. Valverde, and A. Cano, "Effect of a SOFC plant on distribution system stability," *J. Power Sources*, vol. 129, no. 2, pp. 170–179, Apr. 2004.
- [12] A. Nikoobakht, J. Aghaei, M. Shafie-Khah, and J. P. S. Catalao, "Continuous-Time Co-Operation of Integrated Electricity and Natural Gas Systems With Responsive Demands Under Wind Power Generation Uncertainty," *IEEE Trans. Smart Grid*, vol. 11, no. 4, pp. 3156–3170, Jul. 2020.
- [13] H. K. Nguyen, A. Khodaei, and Z. Han, "Incentive Mechanism Design for Integrated Microgrids in Peak Ramp Minimization Problem," *IEEE Trans. Smart Grid*, vol. 9, no. 6, pp. 5774–5785, Nov. 2018.
- [14] N. Valitov, "Risk premia in the German day-ahead electricity market revisited: The impact of negative prices," *Energy Economics*, vol. 82, pp. 70–77, Aug. 2019.
- [15] A. Jiang, H. Yuan, and D. Li, "Energy management for a community-level integrated energy system with photovoltaic prosumers based on bargaining theory," *Energy*, vol. 225, Jun. 2021.
- [16] S. Fan, Q. Ai, and L. Piao, "Bargaining-based cooperative energy trading for distribution company and demand response," *Appl. Energy*, vol. 226, pp. 469–482, Sep. 2018.
- [17] R.-P. Liu, Y. Hou, Y. Li, S. Lei, W. Wei, and X. Wang, "Sample Robust Scheduling of Electricity-Gas Systems Under Wind Power Uncertainty," *IEEE Trans. Power Syst.*, vol. 36, no. 6, pp. 5889–5900, Nov. 2021.
- [18] J. Snoussi, S. B. Elghali, M. Benbouzid, and M. F. Mimouni, "Optimal Sizing of Energy Storage Systems Using Frequency-Separation-Based Energy Management for Fuel Cell Hybrid Electric Vehicles," *IEEE Trans. Veh. Technol.*, vol. 67, no. 10, pp. 9337–9346, Oct. 2018.
- [19] Q. Li, Y. Qiu, H. Yang, Y. Xu, W. Chen, and P. Wang, "Stability-constrained two-stage robust optimization for integrated hydrogen hybrid energy system," *CSEE JPES*, 2020.
- [20] G. Qin, Q. Yan, D. Kammen, C. Shi, and C. Xu, "Robust optimal dispatching of integrated electricity and gas system considering refined power-to-gas model under the dual carbon target," *J. Clean. Prod.*, vol. 371, Oct. 2022.
- [21] J. Lu, T. Liu, C. He, L. Nan, and X. Hu, "Robust day-ahead coordinated scheduling of multi-energy systems with integrated heat-electricity demand response and high penetration of renewable energy," *Renew. Energy*, vol. 178, pp. 466–482, Nov. 2021.
- [22] B. Bagheri and N. Amjady, "Adaptive-robust multi-resolution generation maintenance scheduling with probabilistic reliability constraint," *IET Gener. Transm. Distrib.*, vol. 13, no. 15, pp. 3292–3301, Aug. 2019.
- [23] M. Abeysekera, J. Wu, N. Jenkins, and M. Rees, "Steady state analysis of gas networks with distributed injection of alternative gas," *Appl. Energy*, vol. 164, pp. 991–1002, Feb. 2016.
- [24] F. Liu, Z. Bie, and X. Wang, "Day-Ahead Dispatch of Integrated Electricity and Natural Gas System Considering Reserve Scheduling and Renewable Uncertainties," *IEEE Trans. Sustain. Energy*, vol. 10, no. 2, pp. 646–658, Apr. 2019.
- [25] L. Yang, X. Zhao, and Y. Xu, "A convex optimization and iterative solution based method for optimal power-gas flow considering power and gas losses," *Int. J. Electr. Power Energy Syst.*, vol. 121, p. 106023, Oct. 2020.
- [26] M. Chen, Z. Liang, Z. Cheng, J. Zhao, and Z. Tian, "Optimal Scheduling of FTPSS With PV and HESS Considering the Online Degradation of Battery Capacity," *IEEE Trans. Transp. Electrific.*, vol. 8, no. 1, pp. 936–947, Mar. 2022.
- [27] X. Fang, H. Guo, X. Zhang, X. Wang, and Q. Chen, "An efficient and incentive-compatible market design for energy storage participation," *Applied Energy*, vol. 311, p. 118731, Apr. 2022.
- [28] F. Dababneh and L. Li, "Integrated Electricity and Natural Gas Demand Response for Manufacturers in the Smart Grid," *IEEE Trans. Smart Grid*, vol. 10, no. 4, pp. 4164–4174, Jul. 2019.
- [29] V. Khaligh, A. Ghezelbash, M. Mazidi, J. Liu, and J.-H. Ryu, "P-robust energy management of a multi-energy microgrid enabled with energy conversions under various uncertainties," *Energy*, vol. 271, p. 127084, May 2023.
- [30] N. Tomin, V. Kurbatsky, K. Suslov, D. Gerasimov, E. Serdyukova, and D. Yang, "Flexibility-based improved energy hub model for multi-energy distribution systems," *IET Conference Proceedings*, vol. 2022, no. 3, IET, UK, pp. 409–13, 2022.
- [31] A. Ehsan and Q. Yang, "Coordinated Investment Planning of Distributed Multi-Type Stochastic Generation and Battery Storage in Active Distribution Networks," *IEEE Trans. Sustain. Energy*, vol. 10, no. 4, pp. 1813–1822, Oct. 2019.
- [32] S. Boyd, "Distributed Optimization and Statistical Learning via the Alternating Direction Method of Multipliers," *FNT in Machine Learning*, vol. 3, no. 1, pp. 1–122, 2010.
- [33] D. P. Bertsekas, *Nonlinear Programming*, 2nd ed. Athena-Scientific, 1999.
- [34] R. García, A. Marín, and M. Patriksson, "Column Generation Algorithms for Nonlinear Optimization, I: Convergence Analysis," *Optimization*, vol. 52, no. 2, pp. 171–200, Jan. 2003.
- [35] B. Zeng and L. Zhao, "Solving two-stage robust optimization problems using a column-and-constraint generation method," *Oper. Res. Lett.*, vol. 41, no. 5, pp. 457–461, Sep. 2013.